Available online at www.sciencedirect.com

ScienceDirect

Ceramics International 39 (2013) 8673–8679

CERAMICS INTERNATIONAL

www.elsevier.com/locate/ceramint

Nanostructured SnO_2 thin films for NO_2 gas sensing applications

G.D. Khuspe[a], R.D. Sakhare[a], S.T. Navale[a], M.A. Chougule[a], Y.D. Kolekar[b], R.N. Mulik[a], R.C. Pawar[c], C.S. Lee[c], V.B. Patil[a,*]

[a]*Functional Materials Research Laboratory, School of Physical Sciences, Solapur University, Solapur 413255, Maharashtra, India*
[b]*Department of Physics, Pune University, Pune 411007, Maharashtra, India*
[c]*Department of Materials Engineering, Hanyang University, Ansan 426-791, South Korea*

Received 2 March 2013; received in revised form 12 April 2013; accepted 12 April 2013
Available online 22 April 2013

Abstract

We report the synthesis of nanostructured SnO_2 by a simple inexpensive sol–gel spin coating method using m-cresol as a solvent. This method facilitates rapid synthesis at comparatively lower temperature enabling formation of nanostructures suitable for gas-sensing applications. Various physicochemical techniques have been used for the characterization of SnO_2 thin films. X-ray diffraction analysis confirmed the single-phase formation of tetragonal SnO_2 having crystallite size 5–10 nm. SnO_2 showed highest response (19%) with 77.90% stability toward 100 ppm nitrogen dioxide (NO_2) at 200 °C. The response time of 7 s and recovery time of 20 min were also observed with the same operating parameters. The probable mechanism is proposed to explain the selective response toward nitrogen dioxide. Impedance spectroscopy studies showed that the response to nitrogen dioxide is mainly contributed by grain boundaries. The reproducibility and stability study of SnO_2 sensor confirmed its candidature for detection of NO_2 gas at low concentration (10–100 ppm) and lower operating temperature.

Keywords: Sol–gel synthesis; SnO_2 thin films; Crystal structure; NO_2 sensor; Stability

1. Introduction

An environment friendly n-type semiconductor, SnO_2, has been proved to be an excellent gas sensitive material for detection of toxic, combustible, explosive and harmful gases in both the domestic and industrial applications. In the past decade, extensive research has revealed that the solid-state gas sensors play a crucial role in monitoring the environmental and chemical process, occupational health, safety and medical devices [1]. In comparison with the other solid-state sensors, semiconductor metal oxide based sensors have been widely investigated owing to their small dimensions, low cost, fast response and good recovery speed, and high compatibility with Si-based microelectronics [2,3]. Semiconducting metal oxides, such as ZnO, TiO_2, Fe_2O_3 and NiO have been studied widely and are reported to be sensitive toward certain gas species [4–7].

As far as the gas sensor performance is concerned, the gas sensitivity, selectivity and durability are the most important properties. High gas sensitivity is the key factor in detecting gases at very low concentration as recognized by international standards [8]. The efficiency of semiconductor gas sensor is strongly influenced by nature of surface sites, the electron donor/acceptor properties of gas, the adsorption, the surface reaction and subsequent desorption of the gas species [9–11]. Extensive studies have been reported to improve the gas sensing performances of SnO_2 based sensor, such as adding promoters, doping additives, decreasing grain size, controlling pore and surface defects, etc. [11–13]. It is well-known that the shape and size of SnO_2 have a significant influence on its gas sensing properties. Nanosized particles have high surface to volume ratio and hence are ideal as potential gas-sensing materials.

It is known that high temperature is required to form the SnO_2 single phase with tetragonal structure. However, by employing the sol–gel method, it can be synthesized at relatively lower temperature and short time. The phase formation at lower temperature restricts the crystal growth, favors its application in gas sensing. To the best of our knowledge, the nanostructured SnO_2 prepared by a sol–gel spin coating method using m-cresol

*Corresponding author. Tel.: +91 2172744771x202; fax: +91 2172744770.
E-mail address: drvbpatil@gmail.com (V.B. Patil).

0272-8842/$ - see front matter © 2013 Elsevier Ltd and Techna Group S.r.l. All rights reserved.
http://dx.doi.org/10.1016/j.ceramint.2013.04.047

as a solvent have not been reported so far in gas sensor applications. It is well known that the gas sensing properties of oxide materials are strongly influenced by the surface morphology and grain size. Therefore, one can improve the sensitivity by controlling the grain size and surface morphology. The present study deals with the simple and cost effective synthesis of SnO_2 nanoparticles using sol–gel spin coating method with m-cresol as a solvent. The effect of operating temperature, gas concentration and surface morphology on the NO_2 gas sensing properties of nanostructured SnO_2 were studied. The SnO_2 sensor exhibit highest sensitivity toward NO_2 at lower concentration (10–100 ppm) and lower operating temperature (<300 °C). Other gases such as NH_3, C_2H_5OH, CH_3OH, H_2S, and Cl_2 show low response, indicating high selectivity toward NO_2.

2. Experimental details

A sol–gel synthesis method was used for preparation of SnO_2 wherein the AR grade $SnCl_4 \cdot 5H_2O$ and CH_3OH were mixed and the reaction mixture was stirred vigorously at 60 °C for 1 h, leading to the formation of gel. This gel was further heated for 10 min to obtain faint yellow color powder. The obtained powder was then placed in an alumina boat and annealed at 700 °C for 1 h, subsequently cooled to room temperature. Samples were collected, washed several times with distilled water to remove the salt and dried in air at 100 °C for 1 h. For thin film formation, SnO_2 powder was dissolved in m-cresol and solution was continuously stirred for 11 h at room temperature and filtered. The filtered homogeneous solution of SnO_2 was deposited on to a glass substrate by a single wafer spin coating unit. The above films were characterized by various techniques. The structural and particle size determination was carried out by a Philips PW-3710 X-ray diffractometer using CuK_α line with an accelerating voltage of 40 kV. The Field emission scanning electron microscopy (FESEM) images were scanned using MIRA3 TESCAN, USA while Transmission electron microscopy (TEM) was performed using Philips-800 TEM. The thickness of the film was measured by using AMBIOS XP-1 surface profiler with 1 A° vertical resolution. The detailed gas-sensing characterization was carried out at different operating temperatures and for different gases to explore the applications for these films. Impedance measurements were carried out in the frequency range 20–10 MHz using Wayne Kerr make (model 6500-B) precision impedance analyzer. The measurements were carried out at 200 °C temperature.

3. Gas sensing characteristics

To study the gas-sensing characteristics of SnO_2, samples were made in the thin film form with thickness 0.92 μm [14]. The gas response was measured after providing the ohmic contacts using silver paste. Films were subjected for studying sensitivity and selectivity toward the known amount of various test gases using the custom fabricated dynamic setup [15,16]. The sensor film was kept in the insulated steel chamber. The known amount of test gas was introduced in the gas-mixing chamber so that the required ppm level was attained. The gas-sensing characteristics with reference to time, at different operating temperatures and concentrations were recorded using a programmable 6514 Keithley Electrometer. The gas response (S) for a given test gas is calculated as follows:

$$S = R_a/R_g \quad (1)$$

where R_a and R_g are the electrical resistances of the sensor in air and in test gas, respectively.

4. Results and discussion

Sol–gel spin coating thin film deposition technique offers an important advantages over other techniques due to excellent compositional control, high homogeneity at the molecular level, lower crystallization temperature, large surface area and feasibility of producing thin films on complex shapes. A major advantage of sol–gel processes over other methods is the ability to control the microstructure of deposited film, i.e. the pore size, pore volume [17].

It is well known that the gas response is a surface phenomena wherein, various oxygen species viz., O^-, O^{2-} and O^{2-} available on the surface of metal oxide play a significant role in the detection of gases. More precisely, depending upon the temperature, oxygen is ionosorbed on the surface primarily as O^{2-} ions below 147 °C or as O^- ions between 147 °C and 397 °C. Above 397 °C, the formation of O^{2-} also occurs, which then directly gets incorporated into the lattice above 597 °C [18].

4.1. Structural characterization

Fig. 1 shows the XRD patterns of SnO_2 without any impurity phase. All the diffraction patterns show characteristic SnO_2 peaks with tetragonal structure (JCPDS no. 72-1147). The lattice parameters calculated for the tetragonal phase of SnO_2 using Eq. (2) has been found to be $a=b=0.47$ nm and $c=0.33$ nm which is in good agreement with the reported

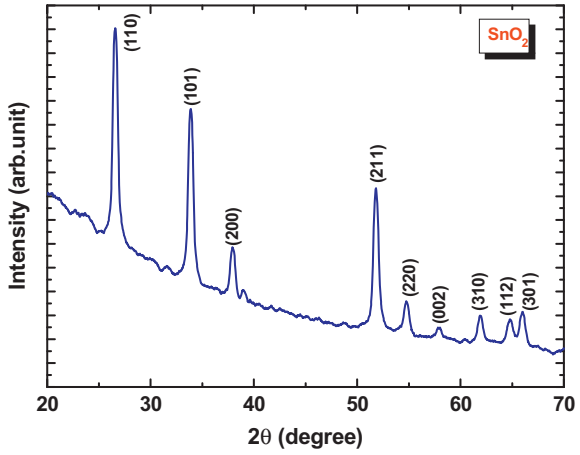

Fig. 1. XRD pattern of SnO_2 calcinated at 700 °C.

JCPDS no. 72-1147.

$$1/d^2 = h^2 + k^2/a^2 + l^2/c^2 \quad (2)$$

The average crystallite size (D) calculated from Scherer's formula, Eq. (3) is in the range of 10–15 nm.

$$D = 0.94\lambda/\beta \cos\theta \quad (3)$$

where 'D' is the average crystallite size, assuming particles to be spherical $K = 0.94$, 'λ' is the wavelength of X-ray radiation, 'β' is the full width at half maximum of the diffracted peak measured in radians and θ is the angle of diffraction.

4.2. FESEM analysis

The two-dimensional high magnification surface morphology of SnO_2 thin films processed at 700 °C was carried out using FESEM image (Fig. 2). From the FESEM image, it is seen that the film consists of nanocrystalline grains with uniform coverage of the substrate surface with randomly oriented morphology. It is well known that the sensing mechanism is surface controlled process in which grain size, surface states, porosity and oxygen adsorption plays a fundamental role.

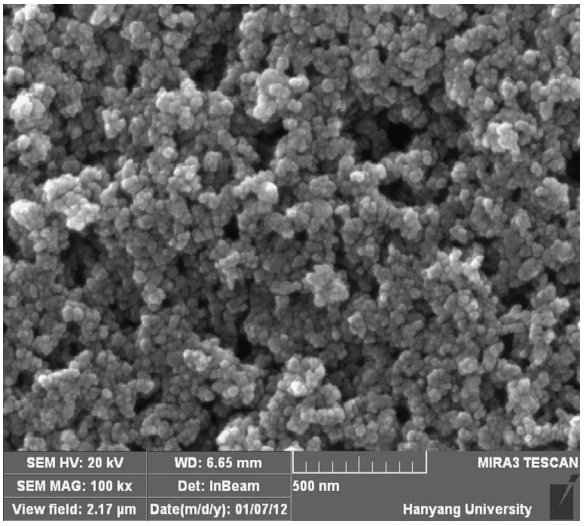

Fig. 2. FESEM of SnO_2 thin films.

4.3. TEM analysis

The shape and size of the nanostructures are determined by TEM. The TEM images of the SnO_2 show formation of nearly nanospherical particles (Fig. 3). It is interesting to find such nanospherical particles remaining distinctly separated even after heating at a high temperature (700 °C). The diameter of particles (Fig. 3(a)) varies from 5 to 10 nm with majority of particles having less than 10 nm size. The selected area electron diffraction (SAED) pattern (Fig. 3 (b)) of an isolated particle shows bright spots corresponding to the (110), (101), (200), (211), (220), (002) lattice planes of a tetragonal structure of SnO_2. These lattice planes match well with the planes observed in the XRD pattern.

Structural studies reveal the formation of large amount of uniformly distributed distinct nanoparticles of SnO_2. Such morphology is preferred for gas sensing, as it promotes adsorption of gas molecules through the film surface.

4.4. Gas-sensing characterization

Gas sensitivity is greatly influenced by the operating temperature. Wide band gap oxides like SnO_2, TiO_2 and ZnO mostly sense gases at higher operating temperatures. The gas response of the samples was tested for the different gases. Prior to gas-sensing characterization, the samples were treated in air at 100 °C for 1 h. This thermal treatment creates oxygen species in the form of O^-, O^{2-} and O^{2-} on the oxide surface which play an important role in the gas-sensing phenomena.

4.4.1. Stabilization of sensor resistance

Stabilization of metal oxide film resistance in ambient air prior to exposure of gas is very important, because it ensures stable zero level for gas sensing application [4,5]. Because of that before exposing gas to SnO_2 films, the electrical resistance

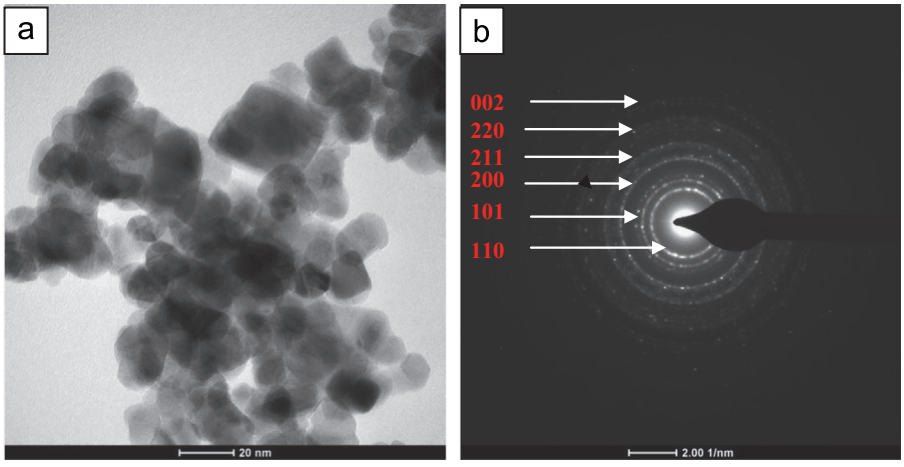

Fig. 3. (a) TEM image of SnO_2 and (b) SAED pattern.

was allowed to be stable for 30 min and the behavior of resistance was observed. Fig. 4 shows the initial stabilization curve of the SnO_2 film at 200 °C. The decrease in resistance observed at the beginning of stabilization period can be attributed to the generation of electrons due to thermal excitation [4,5]. The resistance of the film decreases gradually from 1.60×10^9 Ω to 3.44×10^8 Ω at 200 °C in the first 3 min and for next 6.5 min, the resistance decreases slowly then it remains constant. After 30 min, the SnO_2 thin film attains a stable constant resistance of 4.95×10^8 Ω at 200 °C.

4.4.2. *Effect of operating temperature and NO_2 concentration*

Before exposing to NO_2 gas, the SnO_2 film was allowed to be stable for electrical resistance for 30 min and the stabilized resistance was taken as R_a. Initially, the gas response to 100 ppm of SnO_2 was measured as a function of operating temperature for SnO_2 film and is shown in Fig. 5. The sensor response reached maximum at 200 °C (gas response = 19%) and then decreased. It is well known that at lower temperature, the response is restricted by the speed of chemical reaction, and at high temperature, by the speed of diffusion of gas molecules. At some intermediate temperature, the speeds of two processes become equal, and at that temperature, the sensor response reaches to its maximum [7,8].

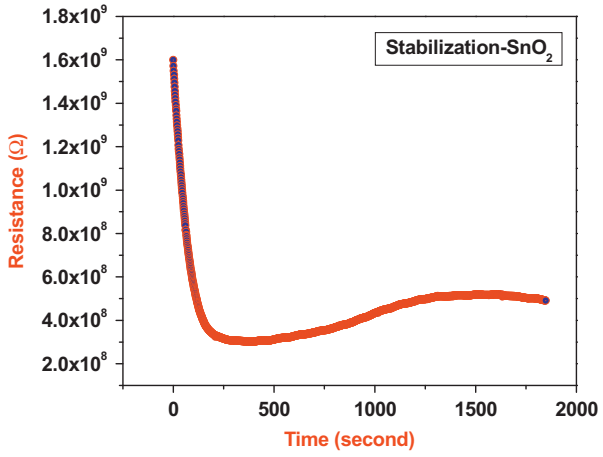

Fig. 4. Resistance stabilization curve with time for SnO_2 film at 200 °C.

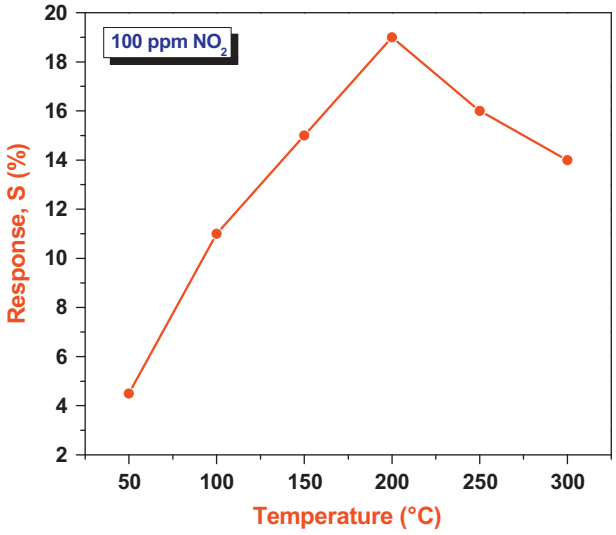

Fig. 5. Response toward NO_2 for SnO_2 at the different operating temperatures.

4.4.3. *Selectivity of SnO_2 sensor*

The ability of a gas sensor to response to a certain gas in the presence of other gases is known as selectivity. The selectivity of a sensor in relation to a definite gas is closely associated with its operating temperature. Fig. 6 shows the bar diagram of gas response of different gases at a fixed concentration of 100 ppm. From the bar diagram, it is revealed that the SnO_2 sensor offered maximum response to NH_3 (4%), H_2S (9%), and NO_2 (19%) at 200 °C. The SnO_2 film showed more selectivity for NO_2 over H_2S compared to NH_3 ($S_{NO2}/S_{H2S} = 2.12$, and $S_{NO2}/S_{NH3} = 4.17$) at an operating temperature 200 °C. It is revealed that NO_2 is more selective against NH_3 and poor selective against H_2S. Different gases have different energies to react with surface of sensor material. The rate of reaction of NO_2 molecules with surface of SnO_2 could be greater. Therefore SnO_2 shows maximum gas response to NO_2 than other gases. Therefore, further dependence of NO_2 response on NO_2 concentration of SnO_2 film was studied.

Once the operating temperature is fixed, the sensor response is studied at different NO_2 concentrations. Fig. 7 shows the response of SnO_2 film as a function of NO_2 concentration. The response increased from 4 to 19%, as the NO_2 concentration increased from 10 to 100 ppm. The gas response showed saturation at NO_2 concentration more than 100 ppm due to increased surface reaction [18,19]. The response of a sensor depends on removal of adsorbed oxygen molecules by reaction with a target gas and generation of electrons. For a small concentration of gas, exposed to a fixed surface area of a sample, there is lower coverage of gas molecules on the surface and hence lower surface reaction occurred. An increase in gas concentration increases the surface reaction due to larger surface coverage [20].

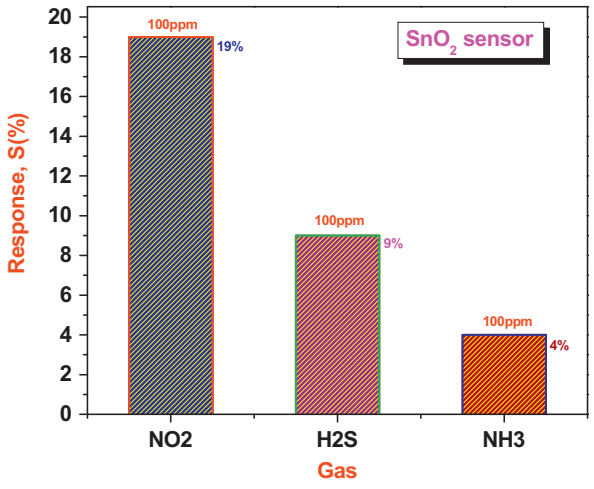

Fig. 6. Gas response of SnO_2 sensor to 100 ppm of NO_2, H_2S and NH_3.

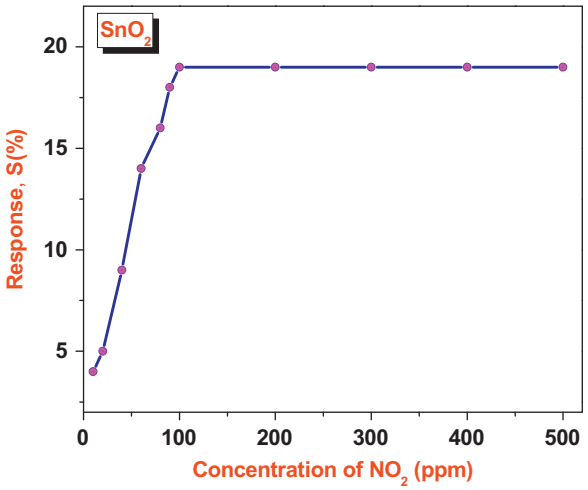

Fig. 7. Variation of gas response of SnO_2 film with different concentrations of NO_2.

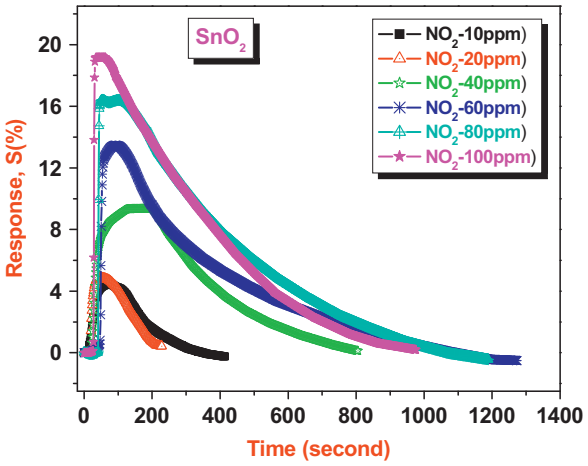

Fig. 8. Dynamic response of SnO_2 sensor for 10–100 ppm NO_2.

4.4.4. Dynamic response of SnO_2 thin films

Fig. 8 shows the dynamic response of SnO_2 sensor with time at 10–100 ppm of NO_2 at 200 °C. From Fig. 8, it is observed that the response increased from 4 to 19% with increasing the gas concentration of NO_2 from 10–100 ppm. At 100 ppm, the SnO_2 sensor showed the maximum response of 19%. Such a maximum response is due to interactions between the NO_2 gas and the surface of SnO_2 film. So, it is obvious that for the materials of greater surface area, the interactions between the adsorbed gases and the sensor surface are significant [21].

4.4.5. Response and recovery times of SnO_2 films

The response/recovery time is an important parameter used for characterizing a sensor. The response time is defined as the time at which the resistance of the SnO_2 thin film reaches to 90% of the saturation value on exposure to NO_2 and the recovery time is defined as the time required for recovering the 90% of the original resistance [21–23]. The variation of response and recovery time with different concentrations of NO_2 at operating temperature 200 °C is shown in Fig. 9. It is observed that the response time decreased from 30 to 7 s while recovery time increased from 302 to 1202 s as the NO_2 concentration increased from 10 to 100 ppm. The decrease in response time may be due to the large availability of vacant sites on the film for gas adsorption as evident from FESEM and TEM images and increase in the recovery time may be due to the heavier nature of NO_2 and the reaction products are not leaving from the interface immediately after the reaction resulting in decrease in desorption rate.

4.4.6. Reproducibility of SnO_2 sensor to NO_2

The sensor reliability is strongly dependent on the reproducibility and stability exhibited by the sensor material. The reproducibility of SnO_2 sensor was measured by repeating the response measurement a number of times. Fig. 10 depicts the dynamic response transients for different samples of SnO_2 toward NO_2. It is clear that response of the material is almost constant confirming the reproducibility of sensor material.

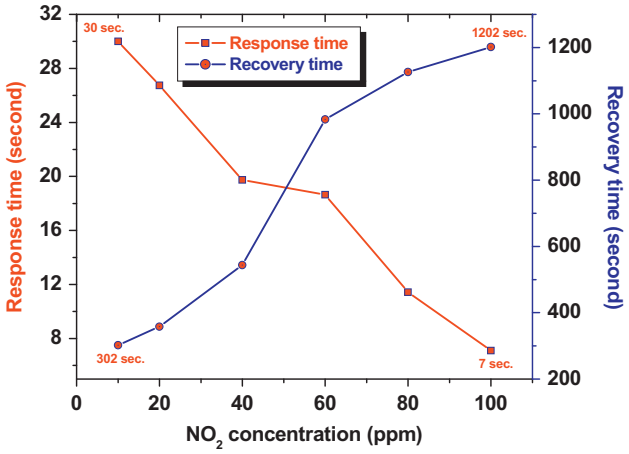

Fig. 9. Variation of response and recovery time of SnO_2 with NO_2 concentration.

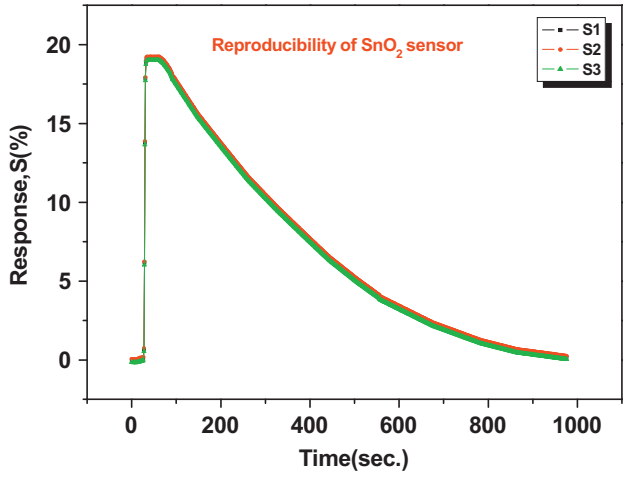

Fig. 10. Reproducibility of SnO_2 sensor at 100 ppm NO_2.

4.4.7. Stability of SnO_2 sensor

Reproducibility and stability of the SnO_2 sensor were measured by repeating the test many times. During the test, no significant variation was observed and is shown in Fig. 11. The obtained results show that both sensitivity and electrical conductance are reproducible. In order to determine the stability of SnO_2 sensor, the response of sensor was tested at fixed concentration of 100 ppm and temperature (200 °C) of NO_2 for 45 days in an interval of 5 days. Initially SnO_2 sensor shows relatively maximum response, however it is dropped from 19% to 14.8% and stable response obtained after 15 days with 77.90% stability. This is because in the initial stage SnO_2 sensor may undergo interface modification during operation and then reaches to steady state indicating the stability of SnO_2 sensor operating at 200 °C temperature.

4.4.8. Impedance spectroscopy studies

Impedance measurements were performed on SnO_2 film before and after exposure to NO_2. The results are shown in Fig. 12 in the form of cole–cole plot. The impedance spectra were analyzed

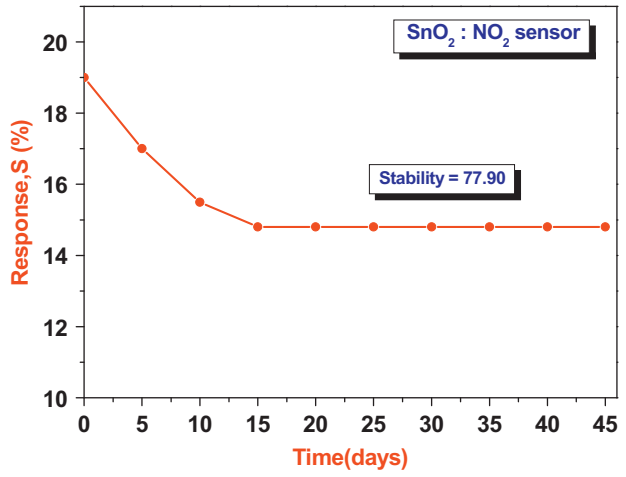

Fig. 11. Stability of SnO_2 thin film sensor at 100 ppm NO_2.

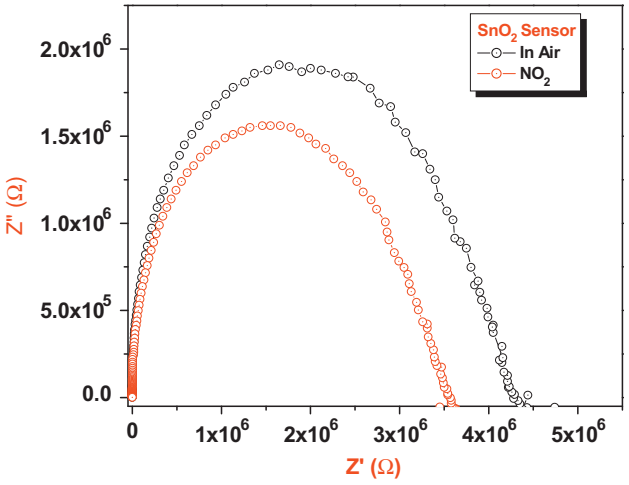

Fig. 12. Impedance spectra of SnO_2 film before and after exposure to NO_2 at 200 °C.

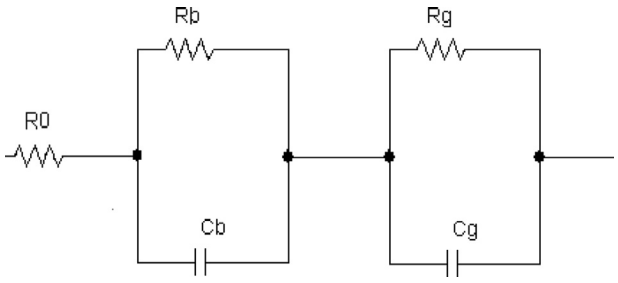

Fig. 13. Equivalent circuit used to interpret the impedance spectroscopy data obtained for SnO_2 films.

Table 1
Parameters obtained by fitting experimental data of impedance spectroscopy to equivalent circuit.

Ambient	R_0 (MΩ)	R_b (MΩ)	C_b (nF)	R_g (MΩ)	C_g (nF)
Unexposed(air)	3.4	0.5	0.231	10.2	224
Exposed to NO_2	2	0.1	0.287	5.7	12.4

using equivalent circuit shown in Fig. 13 [24]. Here R_0 is dc resistance, which is independent of frequency and is attributed to the bulk and surface contributions to the total resistance. R_b and C_b are the resistance and capacitance of intragrain (bulk) region while R_g and C_g are the resistance and capacitance of grain boundary region. Curves obtained by fitting of experimental data to the equivalent circuit are also shown in Fig. 12. A good agreement of the data with theoretical curve is observed. Values of various parameters of the equivalent circuit obtained by curve fitting are given in Table 1. It is seen that on exposure to NO_2, the bulk resistance R_b of the film decreases more than four times while the grain boundary resistance R_g decreases more than two times indicating that both grain boundary and intragrain (bulk) regions contribute to gas sensitivity.

We may have the semiconducting SnO_2 (n-type) grains separated by intergrain region having significant fraction of O_2, adsorbed oxygen and defects. This adsorbed oxygen at grain boundaries traps electrons from grains of SnO_2 reducing carrier density of n-type material and depressing the electron transport. Decrease in electron density in the intragrain region is more significant near the interface. This decreases the conductivity in both the regions. The removal of adsorbed oxygen (acceptors) by NO_2 leads to an increase in the majority carrier density and thus decreasing the resistivity of film.

5. Conclusion

Sol–gel spin coating technique was employed for fabrication of nanostructured SnO_2 thin film sensor on glass substrate. This process is convenient, environment friendly and effective for making nanosized material. Structural studies revealed the formation of tetragonal SnO_2. Microstructural analysis confirms nanostructured morphology suitable for gas sensing application. The gas sensing measurements at 200 °C showed that SnO_2 film is selective at low concentration of NO_2 gas.

SnO_2 thin film sensor exhibits maximum response of 19% with 77.90% stability toward NO_2 gas. Impedance spectroscopy studies revealed that the change in resistance of the SnO_2 film after exposure to NO_2 is mainly contributed by intragrain region. The gas sensing characteristics viz, selectivity, response reproducibility and stability showed that SnO_2 would be a prospective candidate for the detection of NO_2 gas at low concentration (10–100 ppm) and at lower operating temperature.

Acknowledgments

Authors are grateful to the Department of Atomic Energy-Board of Research in Nuclear Science, Govt. of India, New Delhi for Financial support through the scheme no. 2010/37P/45/BRNS/1442.

References

[1] N. Barsan, D. Koziej, U. Weimar, Metal oxide-based gas sensor research: how to?, Sensors and Actuators B: Chemical 121 (2007) 18–35

[2] T.J. Hsueh, C.L. Hsu, S.J. Chang, I.C. Chen, Laterally grown ZnO nanowire ethanol gas sensors, Sensors and Actuators B: Chemical 126 (2007) 473–477.

[3] T.J. Hsueh, S.J. Chang, C.L. Hsu, Y.R. Lin, I.C. Chen, Highly sensitive ZnO nanowire ethanol sensor with Pd adsorption, Applied Physics Letters 91 (2007) 053111–053113.

[4] M.A. Chougule, S.L. Patil, S.G. Pawar, B.T. Raut, P.R. Godse, Shashwati Sen, V.B. Patil, Fabrication of nanostructured ZnO thin film sensor for NO_2 monitoring, Ceramics International 28 (2012) 2685–2692.

[5] S.G. Pawar, M.A. Chougule, B.T. Raut, P.R. Godse, S.A. Pawar, Shashwati Sen, V.B. Patil, Nanocrystalline TiO_2 thin films: NH_3 monitoring and physical characterization, Journal of Materials Science Materials in Electronics 23 (2012) 273–279.

[6] S.T. Navale, S.R. Nalage, M.A. Chougule , S.A. Pawar, V.B. Patil, Novel process for synthesis of α-Fe_2O_3: microstructural and optoelectronic investigations, Journal of Materials Science Materials in Electronics, 24 (2013) 1422–1430.

[7] S.R. Nalage, M.A. Chougule, Shashwati Sen, V.B. Patil, Fabrication and characterization of nickel oxide NO_2 sensor, Journal of Materials Science Materials in Electronics 24 (2013) 368–375.

[8] S.T. Navale, D.K. Bandgar, S.R. Nalage, G.D. Khuspe, M.A. Chougule, Y.D. Kolekar, Shashwati Sen, V.B. Patil, Synthesis of Fe_2O_3 nanoparticles, for nitrogen dioxide gas sensing applications, Ceramics International (2013)http://dx.doi.org/10.1016/j.ceramint.2013.01.074.

[9] J. Xu, Q. Pan, Y. Shun, Z. Tian, Grain size control and gas sensing properties of ZnO gas sensor, Sensors and Actuators B 66 (2000) 277–279.

[10] C. Bose, P. Thangadurai, S. Ramasamy, Grain size dependent electrical studies on nanocrystalline SnO_2, Materials Chemistry and Physics 95 (2006) 72–78.

[11] S. Gupta, R.K. Roy, M. PalChowdhury, A.K. Pal, Synthesis of SnO_2/Pd composite films by PVD route for a liquid petroleum gas sensor, Vacuum 75 (2004) 111–119.

[12] Y. Liu, E. Koep, M.L. Liu, A highly sensitive and fast-responding SnO_2 sensor fabricated by combustion chemical vapor deposition, Chemistry of Materials 17 (2005) 3997–4000.

[13] D.L. Chen, L. Gao, Novel synthesis of well-dispersed crystalline SnO_2 nanoparticles by water-in-oil microemulsion-assisted hydrothermal process, Journal of Colloid and Interface Science 279 (2004) 137–142.

[14] R.D. Sakhare, G.D. Khuspe, S.T. Navale, R.N. Mulik, R.C. Pawar, C.S. Lee, M.A. Chougule, V.B. Patil, Nanocrystalline SnO_2 thin films: structural, morphological, electrical transport and optical studies, Journal of Alloys and Compounds 563 (2013) 300–306.

[15] M.A. Chougule, S.G. Pawar, S.L. Patil, B.T. Raut, V.B. Patil, Polypyrrole thin films: room temperature ammonia sensor, IEEE Sensors Journal 11 (9) (2011) 2137–2141.

[16] G.D. Khuspe, D.K. Bandgar, V.B. Patil, Fussy nanofibrous network of polyaniline (PANi) for NH_3 detection, Synthetic Metals 162 (2012) 1822–1827.

[17] S.L. Patil, S.G. Pawar, A.T. Mane, M.A. Chougule, V.B. Patil, Nanocrystalline ZnO thin films: optoelectronic and gas sensing properties, Journal of Materials Science Materials in Electronics 21 (2010) 1332–1336.

[18] M.S. Tong, G.R. Dai, D.S. Gao, Surface modification of oxide thin film and its gas-sensing properties, Applied Surface Science 171 (2001) 226–230.

[19] S. Saito, M. Miyayama, K. Kaumoto, H. Yanagida, Gas sensing characteristics of porous ZnO and Pt/ZnO ceramics, Journal of the American Ceramic Society 68 (1985) 40–43.

[20] E. Traversa, New ceramic materials for chemical sensors, Journal of Intelligent Materials Systems and Structures 6 (1995) 860–869.

[21] M.A. Chougule, S.G. Pawar, P.R. Godse, R.D. Sakhare, Shashwati Sen, V.B. Patil, Sol–gel derived Co_3O_4 Thin films: effect of annealing on structural, morphological and optoelectronic properties, Journal of Materials Science Materials in Electronics 23 (2012) 772–778.

[22] G. Korotcenkov, V. Brinzari, J. Schwank, M. DiBattista, A. Vasiliev, Peculiarities of SnO_2 thin film deposition by spray pyrolysis for gas sensor application, Sensors and Actuators B 77 (2001) 244–252.

[23] B.T. Raut, P.R. Godse, S.G. Pawar, M.A. Chougule, V.B. Patil, Development of nanostructured CdS sensor for H_2S recognition: structural and physical characterization, Journal of Materials Science Materials in Electronics 23 (2012) 956–963.

[24] J.R. Macdonald, Impedance Spectroscopy, Wiley, New York, 1987.